frontiers | Frontiers in Nuclear Engineering

TYPE Original Research
PUBLISHED 15 December 2022
DOI 10.3389/fnuen.2022.1042541

Check for updates

OPEN ACCESS

EDITED BY
David García,
Amphos 21, Spain

REVIEWED BY
Nathalie Mace,
Commissariat à l'Energie Atomique et aux Energies Alternatives (CEA), France
Catherine Landesman,
UMR6457 Laboratoire de Physique Subatomique et des Technologies Associées (SUBATECH), France
Delphine Durce,
Belgian Nuclear Research Centre, Belgium
Svante Hedström,
Swedish Nuclear Fuel and Waste Management, Sweden

*CORRESPONDENCE
M. Felipe-Sotelo,
m.felipe-sotelo@surrey.ac.uk

SPECIALTY SECTION
This article was submitted to Radioactive Waste Management, a section of the journal Frontiers in Nuclear Engineering

RECEIVED 12 September 2022
ACCEPTED 17 November 2022
PUBLISHED 15 December 2022

CITATION
Hinchliff J, Felipe-Sotelo M, Drury D, Evans NDM and Read D (2022), Cellulose degradation products and high ionic strength enhance the retardation of strontium in hydrated cement paste.
Front. Nucl. Eng. 1:1042541.
doi: 10.3389/fnuen.2022.1042541

COPYRIGHT
© 2022 Hinchliff, Felipe-Sotelo, Drury, Evans and Read. This is an open-access article distributed under the terms of the Creative Commons Attribution License (CC BY). The use, distribution or reproduction in other forums is permitted, provided the original author(s) and the copyright owner(s) are credited and that the original publication in this journal is cited, in accordance with accepted academic practice. No use, distribution or reproduction is permitted which does not comply with these terms.

Cellulose degradation products and high ionic strength enhance the retardation of strontium in hydrated cement paste

J. Hinchliff[1], M. Felipe-Sotelo[2]*, D. Drury[3], N.D.M. Evans[4] and D. Read[2]

[1]Department of Chemistry, Loughborough University, Loughborough, United Kingdom, [2]School of Chemistry and Chemical Engineering, University of Surrey, Guildford, United Kingdom, [3]WSP Golder, Stanton-on-the-Wolds, United Kingdom, [4]College of Science and Technology, School of Science and Technology, Nottingham Trent University, Nottingham, United Kingdom

The present concept for the disposal of some low- and all intermediate-level radioactive waste in the United Kingdom involves grouting with cement in steel drums and placement in a geological facility. The vaults would then be backfilled with low strength, high porosity cement-based materials designed to promote a pervasive, alkaline environment in which many of the radioactive species present are sparingly soluble. This work investigates the interaction of strontium with such a backfill under both diffusive and advective conditions given the potential significance of the fission product ^{90}Sr. An important characteristic of the United Kingdom waste inventory is the abundance of organic compounds, including cellulosic materials; consequently, the experiments were repeated with products of alkaline cellulose degradation. Additional experiments were performed at high ionic strength simulating anticipated changes in the salinity of the groundwater. The effective diffusivity (D_e) of strontium in the absence of the organic compounds ranged between 5.5×10^{-11} and 8.5×10^{-11} $m^2 s^{-1}$, with a distribution coefficient (R_d) of between 2.8×10^{-3} and 3.1×10^{-3} $m^3 kg^{-1}$. The presence of organic compounds and/or an increase of ionic strength enhanced the retardation of strontium. The results indicate that the retention of strontium by hydrated cement paste occurs *via* a reversible ion exchange mechanism rather than mineralisation and is promoted by decalcification of the calcium silicate hydrate phases.

KEYWORDS

strontium, through-diffusion experiment, cement, repository backfill, radioactive waste, cellulose degradation products

Introduction

Strontium-90 is a medium-lived ($t_{1/2}$ = 28.8 years), pure beta emitter (E_{max} = 545.9 (14) keV, 100%), generated during nuclear fission in high yield (6%) (Wallace et al., 2012). Cementitious materials are considered good candidates for the retention of ^{90}Sr, because of the close chemical similarities between Ca and Sr. However, owing to the relatively high solubility of $Sr(OH)_2$ (solubility product K_{sp} = 3.2 × 10^{-4}; Ciliberto et al., 2008) in comparison with $Ca(OH)_2$ (portlandite, K_{sp} = 6.45 × 10^{-6};

TABLE 1 Summary of the effective diffusivity (D_e) values and distribution coefficients (R_d) obtained by fitting the through-diffusion experiments for Sr in NRVB with the GoldSim model and comparison with literature values from diffusion and/or leaching studies

Experimental conditions	Sr level	Diffusivity (m^2/s)		Distribution coefficient (m^3/kg)	
		Best fit[a]	Experimental range[b]	Best fit[a]	Experimental range[b]
No-CDP	Tracer	7.0×10^{-11}	$(5.5–8.5) \times 10^{-11}$	3.0×10^{-3}	$(2.8–3.1) \times 10^{-3}$
	Carrier	7.0×10^{-11}	$(6.8–7.2) \times 10^{-11}$	2.4×10^{-3}	$(2.3–2.6) \times 10^{-3}$
CDP	Tracer	7.5×10^{-11}	$(5.5–8.5) \times 10^{-11}$	4.7×10^{-3}	$(4.6–5.1) \times 10^{-3}$
	Carrier	9.3×10^{-11}	$(8.9–9.7) \times 10^{-11}$	3.1×10^{-3}	$(2.8–3.3) \times 10^{-3}$
Gluconate	Tracer	13×10^{-11}	$(11–15) \times 10^{-11}$	5.3×10^{-3}	$(5.0–5.7) \times 10^{-3}$

Literature values

Matrix	Reference	Diffusivity (m^2 s^{-1})	Distribution coefficient (m^3/kg)
Hydrofracture grout	Morgan et al. (1982)	5×10^{-16}	
Portland cement with 5 wt% Na_2SO_4	Fuhrmann et al. (1989)	$(4.4–4.9) \times 10^{-14}$[c]	—
Sulphate resistant Portland cement mortar	Atkinson et al. (1989)	0.6×10^{-12}	—
Sulphate resistant Portland cement concrete		0.41×10^{-12}	—
BFS/OPC mortar		4.0×10^{-9}	—
BFS/OPC concrete		3.2×10^{-10}	—
Lime grout		3.9×10^{-11}	—
Sulphate resistant Portland cement with silica fume	Johnston and Wilmot (1992)	$(1.7–4.0) \times 10^{-13}$	$(0.1–0.19) \times 10^{-3}$
OPC	Krishnamoorthy et al. (1993)	3.5×10^{-13}	—
Concrete (w/c = 0.4)	Castellote et al. (1999)	$(0.2–3.4) \times 10^{-14}$	—
OPC	El-Kamash et al. (2006)	5.4×10^{-12}	—
OPC + 4% zeolite		3.8×10^{-12}	—
CEM II (compacted crushed hardened cement paste)	Kittnerová et al. (2020)	—	9×10^{-3}
OPC	Goo et al. (2021)	7.62×10^{-15}	—
Alite (triclinic C_3S)	Shiner et al. (2022)	$(23 \pm 8) \times 10^{-14}$	—
OPC (CEMI)		$(3 \pm 2) \times 10^{-14}$	—
Low pH formulation 60.8 %wt Alite + 39.2 %wt colloidal silica		$(1.9 \pm 0.7) \times 10^{-14}$	—
Low pH formulation 50 %wt CEMI + 50%wt colloidal silica		$(0.6 \pm 0.2) \times 10^{-14}$	—

[a]Minimisation of the LOF (lack of fit, details in Felipe-Sotelo et al., 2014)
[b]Interval that envelopes the whole experimental data set
[c]Data at 20°C

Duchesne and Reardon, 1995), retention of Sr by a cementitious matrix is less likely to be controlled by solubility restrictions (Atkins and Glasser, 1992). Fuhrmann et al. (1989) reported that leaching of Sr from Portland cement paste with 5 wt% sodium sulphate is controlled by exchange and diffusion processes rather than by mineral dissolution. A later study by Tits et al. (2004), looking into interactions with a specific cementitious phase, calcium silicate hydrate (CSH), also concluded that co-precipitation processes do not contribute to the retention of Sr^{2+} by CSH phases. However, partial substitution of Ca atoms by Al in the structure of tobermorite (a crystalline form of CSH) has been shown to cause an increase in Sr retention and reduced leachability of Sr from ordinary Portland cement (OPC) (Shrivastava and Verna, 1995; Shrivastava and Shrivastava, 2000, 2001).

The comprehensive study presented by Atkins and Glasser (1992) established that the majority (more than 99%) of any Sr added to cementitious matrices is retained by substitution of Ca in hydrate phases. They believed that calcium (sulfo-) aluminate phases (AF_t and C_3AH_6) are responsible for most of the Sr retention, followed to a lesser extent by CSH. Thus, Shiner et al. (2022) found lower diffusivities of Sr in OPC and low pH-OPC formulations (50%wt OPC +50%wt colloidal silica) when compared with model systems based in alite ($3CaO{\cdot}SiO_2$ or C3S in cement chemistry notation) or alite with colloidal silica alone (Table 1). The authors attributed the reduced mobility of Sr to the presence of ettringite (AF_t) in the OPC systems and the ability of Sr to substitute Ca in the crystal lattice. Nevertheless, since CSH is the most abundant cementitious mineral, constituting 50 wt% in hydrated Portland cement paste (Gaona et al., 2011), much attention has been focussed on studying the uptake of Sr by this phase (Tits et al., 2004; Tits et al., 2006; Wieland et al., 2008; Youssef et al., 2014; Dezerald et al., 2015; Kittnerová et al., 2020) as well as by its crystalline analogue (tobermorite) (Ma et al., 1996; Coleman et al., 2006; Tits et al., 2006; Tsutsumi et al., 2014; Yarusova et al., 2014; Youssef et al., 2014). Tits et al. (2006) concluded that the uptake of Sr by CSH phases can be described by a Sr^{2+}-Ca^{2+} ion exchange, as they observed a decrease of Sr^{2+} retention with an increase in the Ca:Si ratio of the CSH. The authors concluded that those experimental results could be explained by the competition between Ca^{2+} and Sr^{2+} ion for sorption sites (Tits et al., 2006). Further work carried out by Wieland et al. (2008) on the uptake of ^{90}Sr by hydrated sulphate resistant Portland cements found that, in addition to the Sr^{2+}-Ca^{2+} exchange mechanism, isotopic exchange of radio-strontium with non-radioactive Sr carrier also has a significant effect. The structural model used to explain the EXAFS (extended X-ray absorption fine structure) patterns of Sr bound in both a CSH phase and cement pastes, suggests that CSH controls the Sr uptake in the latter (Wieland et al., 2008).

Atomistic modelling studies have been carried out with the aim of determining the nature of the exchange sites occupied by Sr in the CSH phases as well as the effect of substitution by ^{90}Sr (Youssef et al., 2014) and transmutation into ^{90}Y and ^{90}Zr (Dezerald et al., 2015) on the mechanical properties of the gel. The simulations indicated that substitution is favoured on both the interlayer and polyhedral sites of the CSH; however, the former positions are slightly more stable (Youssef et al., 2014; Dezerald et al., 2015). It was determined that, although substitution by ^{90}Y was energetically favourable, this is not the case for ^{90}Zr, and more importantly, the formation of stable ^{90}Zr interferes with the silicon layers, damaging the mechanical properties of the CSH (Dezerald et al., 2015).

A study by Merz et al. (1987) reported that Sr was retained in the gel pores of hydrated cement pastes and concrete, since there was no evidence of any specific strontium-containing mineral. They concluded that the cementitious matrix acted merely as a physical barrier for Sr migration and that the porosity of the matrix was the most important factor controlling its leachability. This conclusion agrees with research conducted by Johnston and Wilmot (1992) who reported a decrease in Sr leaching from sulphate resistant Portland cement paste, with the addition of increasing amounts of silica fume, or from OPC after the addition of 4% zeolite; in each case, the silicates reduced pore and capillary volumes (El-Kamash et al., 2006). A hypothesis that reconciles concepts of both physical and chemical retention is that the addition of pozzolanic/Si-rich materials to cement not only reduces its porosity but also boosts the amount of SiO_2, which in turn will increase the formation rate of CSH available for Sr uptake (Putero et al., 2013).

The present concept for the disposal of long-lived low- and intermediate-level radioactive waste (LLW/ILW) in the United Kingdom involves conditioning the waste in a cementitious matrix and disposing of it in a geological facility, backfilled with a bespoke formulation, such as Nirex Reference Vault Backfill (NRVB) (Nuclear Decommissioning Authority, 2010a). The purpose of the backfill is to condition incoming groundwater to alkaline pH, thereby limiting the solubility of many safety-relevant radionuclides. In addition to pH buffering, the backfill material has been designed with a high porosity to allow the release of gas generated in the disposal facility through *inter alia* decay, radiolysis, chemical reactions, metal corrosion and microbial processes. The cementitious matrix is also intended to furnish a reactive surface to promote retardation of radionuclides by adsorption, incorporation and co-precipitation (Nuclear Decommissioning Authority, 2010a). Anthropogenic organic ligands present in the LLW/ILW, including cellulose degradation products (CDP), may compromise retardation by the hydrated cement paste, either by increasing the solubility of the radionuclides themselves or by modifying the properties of the cementitious matrix (Keith-Roach, 2008; Ochs et al., 2014; Wieland., 2014). The aim of the present work is to investigate the diffusion of Sr through intact monoliths of NRVB and assess the effect of CDP on retardation by this material. Additional experiments were included to evaluate the role of increasing ionic strength on the system as well as the behaviour of Sr under advective flow; the latter simulating re-saturation of the geological disposal facility post closure.

Experimental

Through–diffusion

The through-diffusion experiments were carried out in a radial configuration, adapting the methodology developed by Markovaara-Koivisto et al. (2008) for the diffusion of radionuclides through crystalline rock. This methodology has been used previously with successful results for investigating Cs^+, I^- (Felipe-Sotelo et al., 2014), Cl^- (van Es et al., 2015), Ni^{2+} (Felipe-Sotelo et al., 2016), Se (Hinchliff et al., 2016), Tc (Isaacs et al., 2020), U and Th (Felipe-Sotelo et al., 2017) diffusion through NRVB specimens. A full description of the preparation of the blocks and the NRVB-equilibrated water and CDP solution can be found in Felipe-Sotelo et al. (2014) (compositions of the solutions are summarised in **Table S1** in Supplementary Information). In the case of the experiments carried out in the presence of CDP, the blocks of NRVB were pre-equilibrated in the CDP mixture for a period of 30 or 50 days. Sr diffusion was investigated at two concentrations; at tracer level where only ^{90}Sr (Perkin-Elmer, 14 kBq as $Sr(NO_3)_2$ equivalent to an initial concentration of 1.9×10^{-8} mol dm^{-3}) was added to the central well of the NRVB blocks, and at higher carrier levels where, in addition to 25 kBq of ^{90}Sr, the central wells in the blocks were spiked with 0.15 mol dm^{-3} inactive $Sr(NO_3)_2$ (99+%, for analysis, Acros Organics). The latter is sufficient to ensure a total concentration in solution of 10^{-3} mol dm^{-3} (C_{max}), assuming homogenous distribution of the Sr in the total solution volume of system (200 cm^3 external solution +25 cm^3 pore volume +1.5 cm^3 well). The activity of ^{90}Sr in the solution in contact with the NRVB blocks was determined after ^{90}Y ingrowth (pure β emitter with a maximum energy of 2.28 MeV and half-life of 64.1 h), by liquid scintillation counting (LSC, TRI-CARB 2500 TR Liquid Scintillation Counter, Packard) in the energy range between 250 and 800 keV. The statistical validity of the measurements was ensured by counting each sample for enough time to satisfy the 2σ criterion (targeted value 10,000 counts). Aliquots of 1 cm^3 of solution were mixed with 10 cm^3 of LSC cocktail (Gold Star Multipurpose Liquid Scintillation Cocktail, Meridian) before analysis. Aliquots taken from the diffusion experiments were not replaced by fresh solution.

In addition to the above, where the NRVB blocks were kept in contact with either with NRVB-equilibrated water or CDP solutions, a series of experiments was carried out using gluconic acid as a surrogate for isosaccharinic acid (ISA), the main component of the CDP mixture and often assumed to be the key complexant (Glaus et al., 2008; Glaus and Van Loon, 2008). Although some researchers have expressed concern about the suitability of gluconic acid as an analogue for ISA (Dudás et al., 2017), gluconic acid is also of relevance as it can be used as plasticiser in concrete admixtures (Glaus et al., 2006). The aim of the diffusion experiments in the presence of gluconic acid was to differentiate the effect of the organic compound from the influence of ionic strength, which might also affect retardation when using a CDP mixture, as the solutions of gluconate in NRVB equilibrated water presented a lower ionic strength than the CDP solutions (**Table S1**). For this purpose, a solution of 2.6×10^{-3} mol dm^{-3} D-gluconolactone ($C_6H_{12}O_7$, the lactone form of gluconic acid with no counter ions present, 99%, Acros Organics) was added to the NRVB-equilibrated water to form gluconate and reach a total organic carbon (TOC) concentration of 187 ppm C, equivalent to the TOC concentration measured in the CDP mixture. As for the experiments carried out in the presence of CDP, the NRVB blocks were pre-equilibrated in the gluconate solution for a minimum period of 30 days before spiking with 12.6 kBq of ^{90}Sr (no carrier added) in the central well at the start of the diffusion assays. The ^{90}Sr diffusion experiments at high ionic strength were carried out following two experimental approaches. In the first set of experiments the ionic strength of the solution in contact with the NRVB blocks was increased by addition of NaCl and KCl (50:50) to a total chloride concentration of 0.1 mol dm^{-3} (both 99+%, for Analysis, Acros Organics), and the blocks were left to pre-equilibrate for a minimum of 30 days before the addition in the central well of a 12.2 kBq ^{90}Sr spike (no carrier). The second experimental approach attempted to simulate the intrusion of hypersaline groundwater into the GDF, so for this purpose an ionic strength gradient was generated through the cement, by loading a slurry of NaCl and KCl (0.66 g NaCl and 0.84 g of KCl) together with 12.2 kBq ^{90}Sr into the central well of the NRVB block (no carrier), before submerging it in the cement equilibrated water. Assuming complete equilibration of the NaCl and KCl through the cement-water system, the final concentration expected in solution was 0.1 mol dm^{-3}. All diffusion experiments were carried out in duplicate, and all the blocks were kept in a glove box under N_2-atmosphere to prevent carbonation.

Advection

The migration experiments under advective conditions were carried out in a radial configuration, using the advection rig described in Felipe-Sotelo et al. (2016); the experimental set-up allowed the direct injection of Sr into the central well of the NRVB block. The solution (either NRVB-equilibrated water or CDP) was contained in a N_2-pressurised vessel, maintaining radial flow of solution through the block under CO_2-free conditions. For the advection tests, experiments were carried out only at tracer levels of ^{90}Sr; the activities injected in the system ranged between 12.3 and 12.4 kBq. The solution eluted from the blocks was collected by means of fraction collector (Frac-920, GE

Healthcare), and breakthrough of ^{90}Sr was determined by LSC as described above.

Autoradiography

At the end of the through-diffusion and advection experiments, the migration profiles and distribution of Sr within the NRVB blocks were visualised by autoradiographic imaging of the ^{90}Sr. The hydrated cement monoliths were cut using a diamond-edged circular saw to expose the centre of the blocks. The flat surfaces were then placed onto Eu^{2+}-doped BaFBr storage phosphor autoradiographic plates (Fuji BAS MP 2025, 20 cm × 25 cm) and exposed from 5 h to 5 days depending on the activity of the sample. The plates were developed using a scanning laser-beam (Auto RAD, Packard Cyclone) and the images processed using ImageQuant (version 4) and ImageJ (U.S. National Institutes of Health).

Modelling

Full description of the use of the GoldSim simulations for the diffusion experiments can be found in Felipe-Sotelo et al. (2014). The experimental data were fitted adjusting the R_d (distribution coefficient) to the data at steady state, followed by the D_e (effective diffusion coefficient) to fit the breakthrough and the initial shape of the curve. The two parameters were then readjusted iteratively to minimise the lack-of-fit (LOF, Felipe-Sotelo et al. (2014)). For the advection experiments presented here, the diffusive mass flow rate of a radionuclide between cells was supplemented with an advective mass flow rate. The radionuclide mass flow rate was calculated as the product of the concentration of the radionuclide in the fluid in the cell and the fluid flow rate. The fluid flow rate between cells was kept equal to the measured rate of flow from the cement block and there is therefore conservation of fluid mass. Dispersion occurs in advective flow regimes and a good first approximation for one dimensional transport through a relatively homogeneous medium is that the dispersivity is 10% of the total length of the pathway (Gelhar et al., 1992). As much of the literature relevant to advection is concerned with large scale geological features or industrial processes, it should be noted that the equations used by GoldSim are conventional and scalable. The linked cells in the model exhibit a degree of numerical dispersion that is a function of the number of cells. In particular, the equivalent numerical dispersivity is equal to half the length of 1 cell. By representing the cementitious block with 5 cells numerical dispersivity has been introduced to the model that is equivalent to 10% of the radius of the NRVB block. The diffusion and advection simulation methods described above are mass conservative and assume that NRVB is homogenous and isotropic with regard to transport properties.

Results

Through—diffusion

Figure 1 shows the results of diffusion through NRVB with and without CDP at tracer level (Figure 1A) and with addition of Sr carrier (Figure 1B). In the absence of organics and at tracer level only, breakthrough of Sr occurred after 20 days, followed by a linear increase in concentration over the following 70 days, before stabilising after 250 days, with 50% of the original ^{90}Sr spike still retained in the NRVB. In the presence of CDP at Sr tracer levels (Figure 1A) breakthrough commenced after 25 days, reaching a plateau after 236 days with 60% of the ^{90}Sr retained on the NRVB. For the experiments using inactive Sr carrier, breakthrough and ^{90}Sr retention were similar in the absence of organics to the tracer tests; however, with addition of the CDP, retention decreased in comparison with the tracer experiments, going from 60 to 45%.

Diffusion experiments using tracer levels of ^{90}Sr in the presence of gluconate are shown in Figure 2; breakthrough of ^{90}Sr occurred after 19 days, reaching a stable concentration in solution after approximately 180 days. The retention of ^{90}Sr by the NRVB was 60% of the total activity originally added to the blocks.

For those experiments in which the ionic strength of the solution in contact with the NRVB was increased by addition of 0.1 mol dm^{-3} NaCl:KCl (50:50), the diffusion curves through the NRVB blocks at tracer levels of ^{90}Sr (Figure 3) show breakthrough of Sr after 25 days, followed by a linear increase in the concentration over a period of 62 days, and it can be observed that the diffusion rate slows down after 102 days. The diffusion experiments in an ionic strength gradient were slower and breakthrough was only observed after 42–51 days, depending on the replicate. The increment of the concentration in solution slows down after approximately 115 days, although more data are needed for confirmation. In both cases, retention of ^{90}Sr by the block increased to 60–70% of the activity initially added.

The autoradiography images show that, for all the experiments (Figure 4 and Supplementary Figure S1), ^{90}Sr was homogeneously distributed within the NRVB matrix, regardless of the total concentration of Sr (tracer vs. carrier) or the presence of organic compounds. There is, however, evidence that some of the ^{90}Sr (tracer level) in the gluconate experiments has remained in the central well. Only in the case of the CDP experiments was the activity retained by the blocks higher than in the organic-free experiments, matching the analyses of the solutions (Figure 4).

Advection

For the two replicate advection experiments carried out without addition of organic compounds and at tracer levels, breakthrough of ^{90}Sr was observed after elution of 50 cm^3 of NRVB–equilibrated

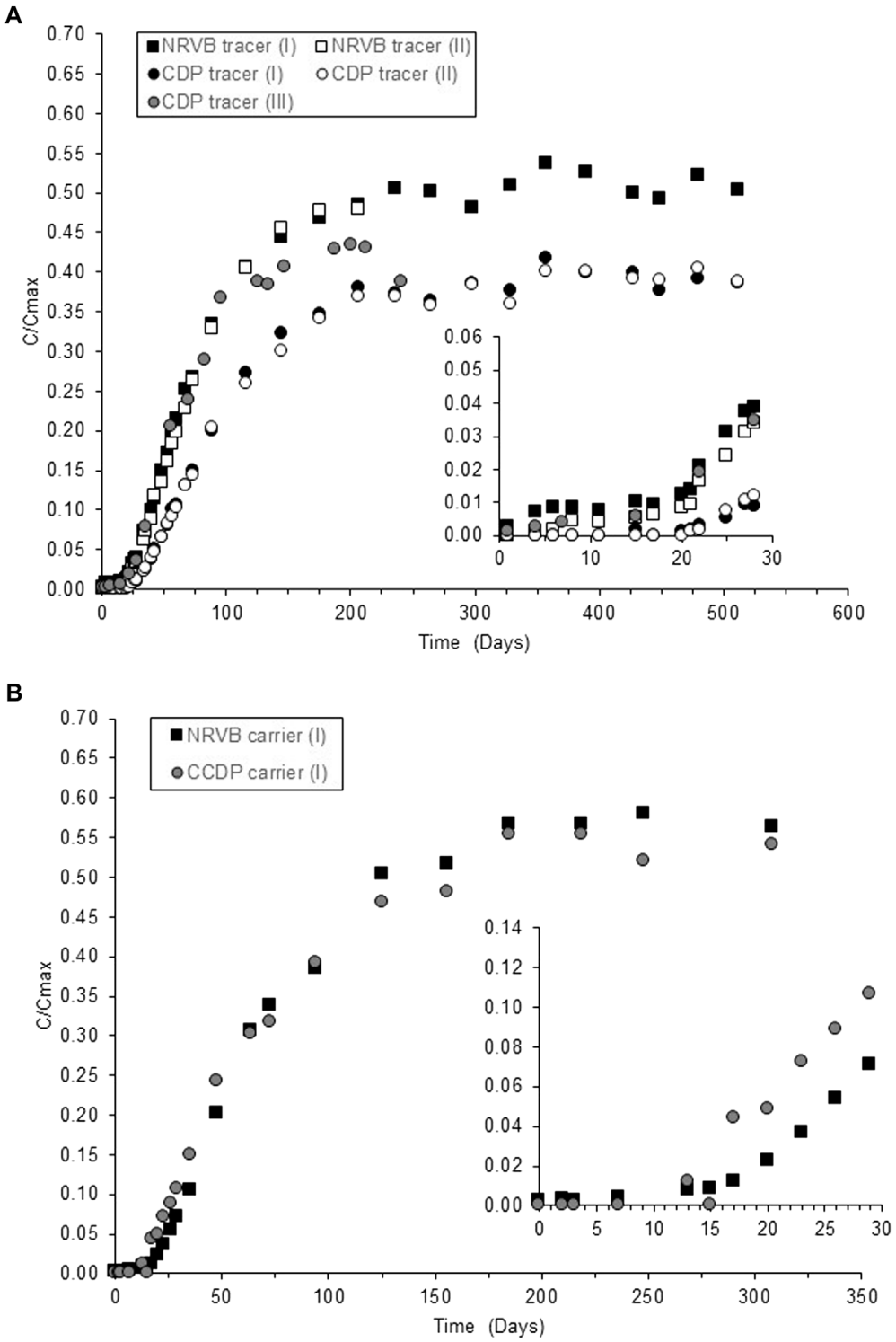

FIGURE 1
Breakthrough curves of Sr through NRVB blocks with and without CDP; **(A)** at tracer and **(B)** carrier levels. C/Cmax represents the ratio between the measured concentration in solution C, and the calculated Cmax, assuming homogenous distribution of the Sr in the total solution volume of the system. Note that for (I) and (II) the pre-equilibration time in the CDP solution before the diffusion experiments was 30 and 50 days for experiment (III).

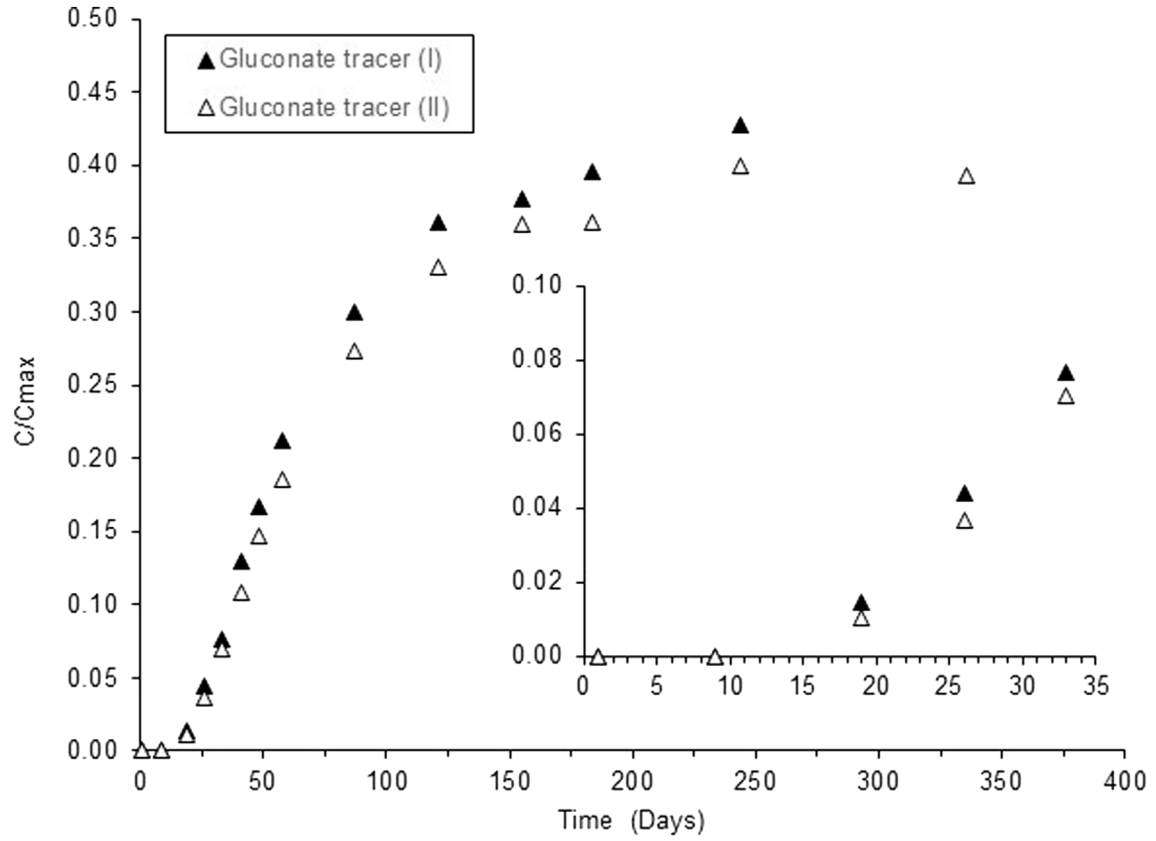

FIGURE 2
Breakthrough curves of Sr through NRVB blocks in the presence of 2×10^{-3} M gluconate at ^{90}Sr tracer levels. C/Cmax represents the ratio between the measured concentration in solution C, and the calculated Cmax, assuming homogenous distribution of the Sr in the total solution volume of the system.

solution (Figure 5), which corresponds to approximately twice the pore volume of the NRVB blocks. The elution profiles in Figure 5 are not complete, as the intention was for some of the ^{90}Sr to remain in the blocks in order to observe its distribution within the cementitious matrix by autoradiographic imaging. An overlap of the breakthrough curves (rising profiles and elution tails) was observed in the absence of organic compounds, notwithstanding fluctuation at the maxima of the elution curves due to malfunction of the fraction collector. Note that the two replicate experiments were carried out on the same specimen.

Clear differences were observed when compared with the elution of ^{90}Sr in the presence of CDP. Breakthrough of the radionuclide occurs sooner when organic compounds are present, after the elution of 42 cm^3 of solution, the profile presents a flatter maximum and more elongated elution tail (Figure 5A). However, when comparing the cumulative recoveries of ^{90}Sr from the NRVB blocks (Figure 5B), it is clear that most of the radionuclide is retained by the solid in the presence of CDP. Further, a lower cumulative recovery was calculated after the same volume of solution had eluted from the blocks (63% vs. 75% recovery, after 250 cm^3 solution). The flat-topped peaks and long tails suggest that dispersion is significant for all experiments, although potentially more pronounced for those with CDP. However, more data would be required to confirm this.

Despite the differences in breakthrough volumes, the retardation behaviour in the advection tests generally corresponds with the results of the diffusion experiments. Differences in breakthrough volume could be due to minor differences in the dimensions of the NRVB blocks or the central well.

The autoradiographic images of the distribution of ^{90}Sr after advection through NVRB in the absence of CDP (Supplementary Figure S2A) show accumulation of the radionuclide in a ring on the outer surface of the block, while the rest of the specimen remains clear of any trace of radioactivity. Only a small residual amount could be detected on the inner walls of the injection well. However, in the presence of CDP, the autoradiography images show higher activity within the cementitious matrix (Supplementary Figure S2B) when similar volumes of solution (200–250 cm ^{3}) had been flushed through the NRVB blocks, consistent with the higher dispersion and sorption.

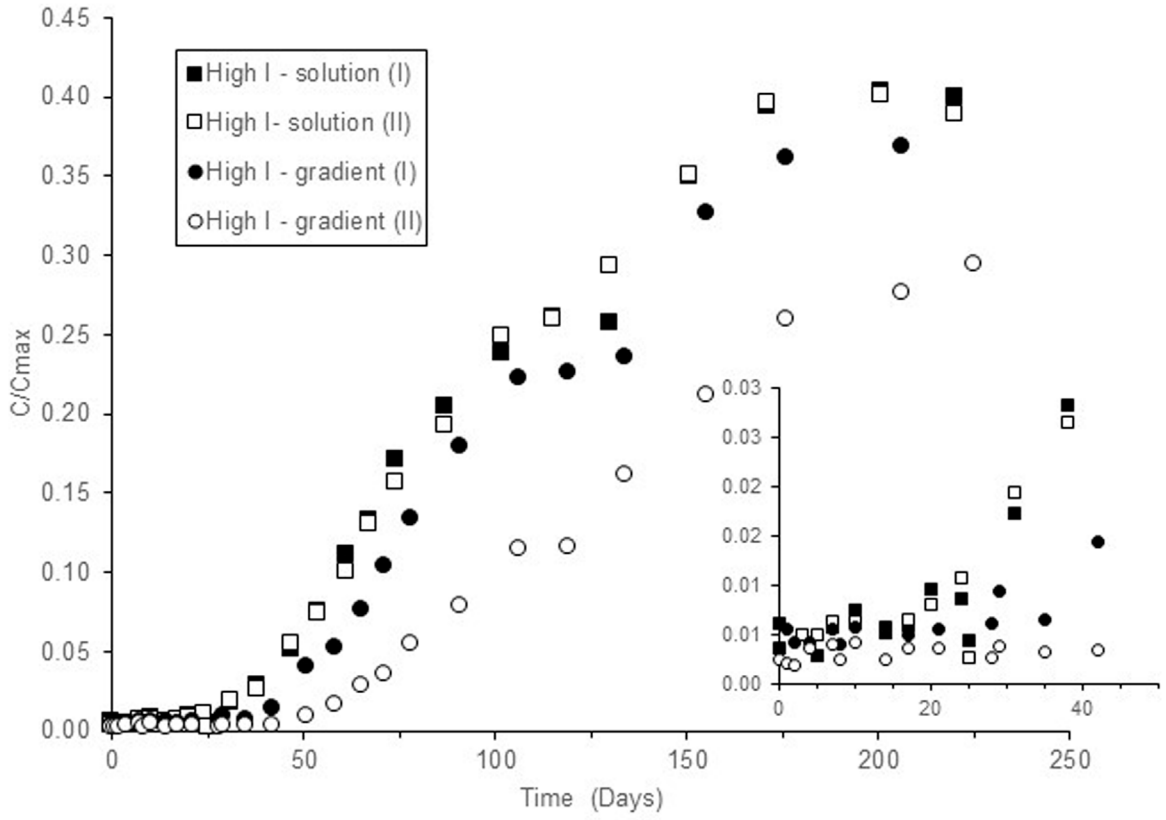

FIGURE 3
Breakthrough curves through NRVB blocks at ^{90}Sr tracer levels in the presence of 0.1 M NaCl + KCl (50:50) added to the NRVB equilibrated water (solution) or added into the block well (gradient). C/Cmax represents the ratio between the measured concentration in solution C, and the calculated Cmax, assuming homogenous distribution of the Sr in the total solution volume of the system.

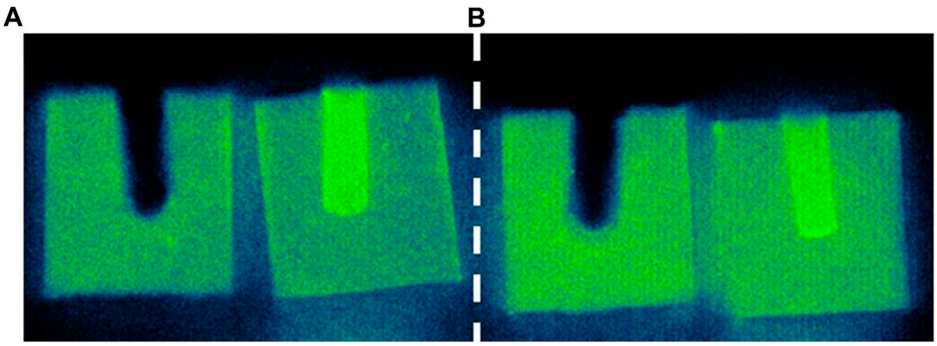

FIGURE 4
Autoradiography images for the distribution of ^{90}Sr within the NRVB blocks corresponding to the through-diffusion experiments at tracer level (no carrier added): **(A)** in the absence of CDP and **(B)** in the presence of CDP. Shine from residual ^{90}Sr in the wells of the blocks can obscure details present in the matrix. Consequently, the well in one-half of each block (fragment located on the left) was plugged with shielding material (modelling clay) resulting in its black appearance in the images.

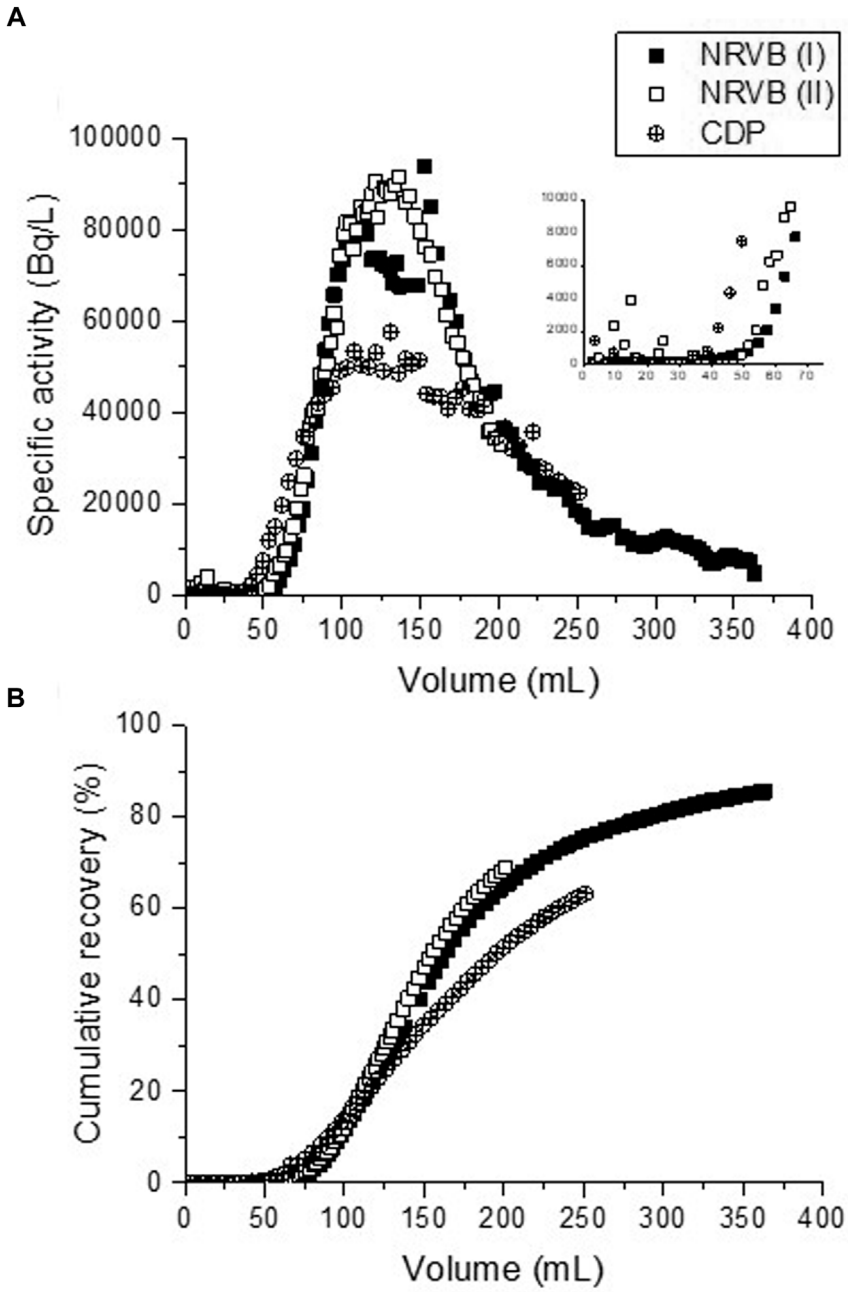

FIGURE 5
(A) Breakthrough curves through NRVB blocks for ^{90}Sr under advective conditions with and without CDP and **(B)** cumulative recoveries of the ^{90}Sr during the advection experiments.

Discussion

Through—diffusion

The results from the through-diffusion experiments were fitted with a GoldSim model (full details regarding the conceptual model and its numerical representation are given in Felipe-Sotelo et al., 2014); the effective diffusivity values (D_e) and distribution coefficients (R_d) are presented in Table 1. The apparent diffusion coefficients (D_a) for a reactive chemical species can be calculated from the effective diffusion attenuated by the R_d and the total porosity (ε), therefore $D_e = \varepsilon R_d D_a$ (Shackelford and Moore, 2013). For all experiments D_e values were lower than for tritiated water (HTO, 0.13–0.17 × 10^{-9} m^2 s^{-1}) used as conservative tracer through

NRVB under similar experimental conditions (Felipe-Sotelo et al., 2014). As observed in Figure 1 and Table 1, the addition of a high concentration of Sr (carrier level) did not result in significant changes in the diffusivity values; however, it reduced retention, which translates to a slight decrease in the distribution coefficients from 3.0×10^{-3} to 2.4×10^{-3} m^3 kg^{-1}, which correspond to site capacity saturation at the experimental concentrations used. This could be explained in terms of the partial saturation of the solid and corresponding reduction in the sites available for the retention of Sr^{2+} either by Sr^{2+}-Ca^{2+} ion exchange (Tits et al., 2006) or isotopic exchange (Wieland et al., 2008). The diffusivity values reported in the literature (Table 1) present a variation of seven orders of magnitude, and in general they seem to show a relationship with the porosity of the hydrated cement paste, i.e. the lower the porosity the lower the diffusivity parameter. Note that the values obtained here for NRVB, in the absence of CDP, fit very well with those previously calculated by Atkinson et al. (1989) for backfill material described in their study as lime grout (3.9×10^{-11} m^2 s^{-1}); this is due to the fact that both backfill materials present a high fractional porosity (approx. 60% as reported by Atkinson et al. (1989), and 55% for NRVB in Nuclear Decommissioning Authority (2010b)). It must be noted that differences in tortuosity and constrictivity between these two materials have not been considered.

From the results in Figure 1, it can be concluded that CDP increase the adsorption of Sr to NRVB, although this effect is reduced in the presence of high concentrations of Sr (i.e. with Sr carrier). The enhanced retardation of Sr in the presence of the CDP could be explained in this ternary system by the retention of the organic species onto the surface of the NRVB, contributing to the immobilisation of Sr by complexation to the organic moiety. Retention of ISA on the surface of cements has been reported previously (Van Loon and Glaus, 1998) as has complexation of Ca by ISA (Vercammen et al., 1999). Owing to the similarities between Ca and Sr, analogous interaction between the CDP and Sr would be expected. However, the fact that the effect of CDP disappears at higher concentrations of Sr suggests that there are other factors affecting the diffusion of Sr in the presence of the organics, such as the ionic strength, background levels (and availability) of Sr in the NRVB and CDP mixture.

In order to differentiate the effect of the organic compound from the influence of ionic strength, the tracer diffusion experiments were repeated with gluconate, an analogue of ISA (Pallagi et al., 2014), at similar TOC levels as in the original CDP mixture. Comparison of the curves in Figure 1A and Figure 2 shows that breakthrough of Sr in the presence of gluconate was slightly faster than with the CDP (19 vs. 25 days), which resulted in higher diffusivity values (7.5×10^{-11} vs. 13×10^{-11} m^2 s^{-1}); however, the relative retention of ^{90}Sr by the NRVB was the same for both sets of experiments, approx. 60%. The increase in diffusivity would indicate that the higher background levels of Sr in the CDP mixtures may have played a role over the time required for breakthrough. The higher concentration of background Sr in the CDP solution (**Table S1**) would result in an initial overall influx of Sr in the NRVB block. Thus, migration of the ^{90}Sr tracer would not start until the Sr concentration gradient between the block and the surrounding solution had subsided. This would suggest that longer equilibration times (more than 30 days) between the NRVB blocks and the CDP solution would be required to obtain reliable and reproducible results. This was also confirmed by an additional experiment in the presence of CDP at ^{90}Sr tracer levels, when the NRVB block was pre-equilibrated with the CDP solution for a period of 50 days before the spiking with ^{90}Sr (Figure 1A, where profiles (I) and (II) correspond to 30-day equilibration and (III) represents the 50-day equilibration experiment).

It is obvious from the results presented in Figure 3 that an increase in the ionic strength, either by addition of salts to the solution in contact with the blocks or by creation of a salinity gradient through the blocks causes a marked reduction in the rate of diffusion through the NRVB as well as increased retention. Johnston and Wilmot (1992) investigated the sorption and diffusion of Sr^{2+} in sulphate resistant Portland cement with and without the addition of silica fume in saline groundwater (0.23 mol dm^{-3} Na^+, 0.85 mol dm^{-3} Cl^-), reporting R_d values in the range 0.1×10^{-3} to 0.19×10^{-3} m^3 kg^{-1}, one order of magnitude lower than the values obtained here. The authors obtained lower distribution coefficients for Sr than expected in comparison with Cs, which was attributed to the high ionic strength of the groundwater (Johnston and Wilmot, 1992). Unfortunately, the authors did not repeat the experiments at lower ionic strength with the same cement formulation to confirm this hypothesis.

It should be highlighted that the effect of an increase in ionic strength is analogous to that observed following the addition of CDP or gluconate. From the work of Tits et al. (2004) and Wieland et al. (2008) it can be concluded that CSH is the solid phase that controls the uptake of Sr^{2+}. Moreover, Tits et al. (2006) made two observations which relate to the present work: 1) Sr uptake onto CSH increases as the Ca:Si ratio in the CSH decreases and 2) the distribution coefficient of Sr onto CSH increases in artificial cement water in comparison to alkali-free solutions. In the current study, organic compounds, either CDP or gluconate, increased the retention of Sr by NRVB. This could be due to the formation of ternary complexes (cement paste-CDP-Sr), where the organic compounds in the CDP interact with both the surface of the cement and the Sr. Despite previous studies reporting little affinity of isosaccharinic or gluconic acids for Sr in alkaline solutions (Evans et al., 2012), the hypothesis of the formation ternary complexes in the CDP-Sr-NRVB system would require further investigation. However, even in the case of limited or no formation of ternary complexes, it is possible that the retention of the CDPs on the cement grout could cause changes of its surface properties. Thus, Tasi et al. (2021) reported that retention of the ISA on the hardened cement paste resulted in alteration of the zeta potential.

Another possible explanation for the effect of the CDP is that the organic compounds complex with Ca in the CSH, effectively reducing the Ca:Si ratio and promoting ion-exchange of Sr on the CSH phases. The effect of a reduction in Ca:Si ratio on the retardation of Sr has been explained by Iwaida et al. (2000) in terms of changes in

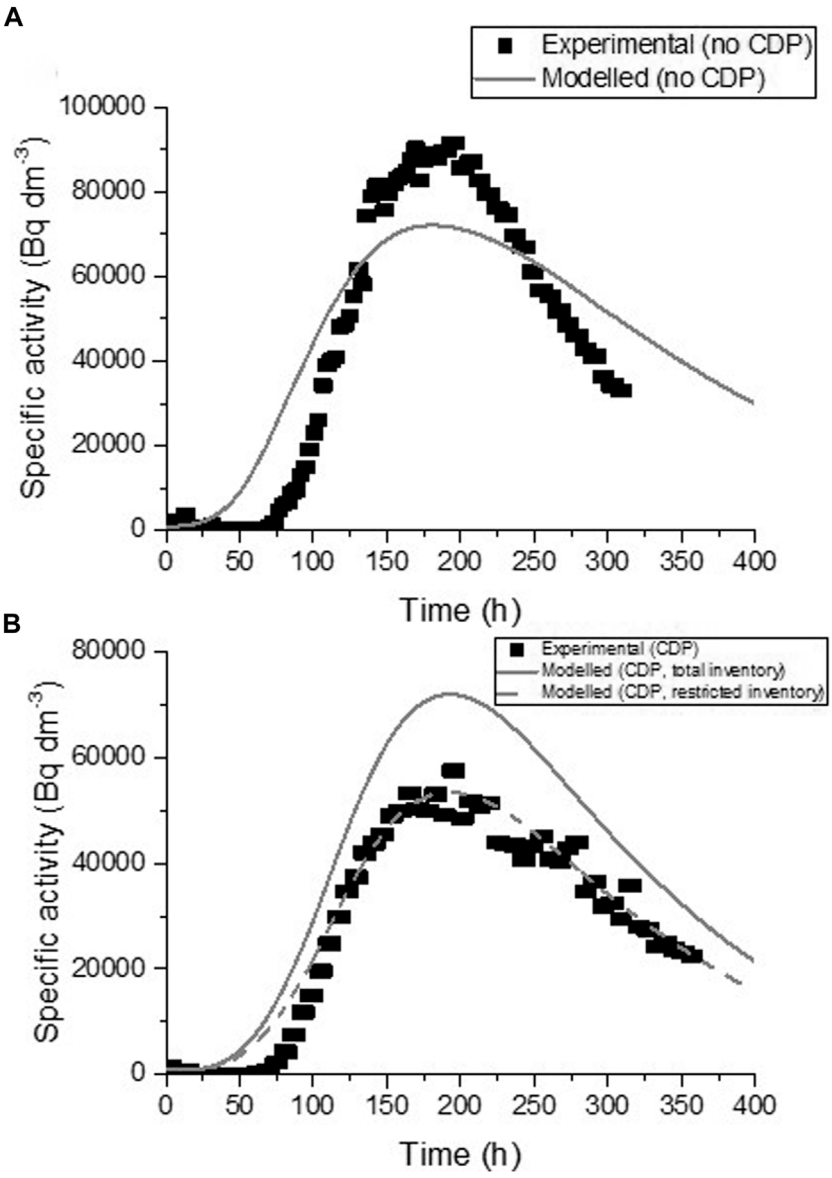

FIGURE 6
Breakthrough curves through NRVB blocks for ^{90}Sr under advective conditions and fitted GoldSim model advection profiles; **(A)** with NRVB-equilibrated water and **(B)** with CDP.

the zeta potential of the CSH phase. As the Ca:Si ratio decreases the zeta potential changes from positive to negative values, corresponding to the dominant groups on the CSH surface changing from $\equiv SiOCaOH_2^+$ or $\equiv SiOCa^+$ to $\equiv SiO^-$; the latter promoting retention of Sr^{2+} by electrostatic adsorption. This also tallies with the hypothesis postulated by Pointeau et al. (2008) when attempting to explain the potential effect of CDP and ISA on the uptake of anionic species by cement pastes, as the formation of Ca-organic species in solution enhances the global negative charge at the surface of the CSH particles, reducing the uptake onto the cement pastes. Similar observations were reported with regards the effect of CDP on the uptake of I^- (Felipe-Sotelo et al., 2014) and Cl^- (van Es et al., 2015) by NRVB.

An increase in ionic strength acts in the same direction as the presence of the organic compounds, increasing the retardation of Sr; Putero and Rosita (2013) point out that saline water accelerates degradation of the cement pastes owing to the following reaction:

$$Ca(OH)_2 + 2NaCl \rightarrow 2NaOH + CaCl_2 \quad (1)$$

This decalcification generates soluble $CaCl_2$ thereby reducing the Ca:Si ratio in the solid and leading to the degradation of the CSH gel (Liu et al., 2014). It can be inferred that decalcification

due to high ionic strength caused the increase in Sr retardation by NRVB in the presence of 0.1 mol dm^{-3} NaCl/KCl solution in the current work. These observations also seem to be in agreement with the work by Gashier et al. (2014), who reported that the introduction of Sr (as $Sr(NO_3)_2$) into 9:1 blast furnace slag:OPC blends resulted in inhibition of Portlandite formation and an increase of the leaching rate of Ca^{2+}.

In the case of CDP mixtures, which contain not only organic compounds but also show higher ionic strengths than pure cement-equilibrated waters, it is not possible to establish which of the two effects predominates. The experimental evidence along with data from previous studies suggests that the effects operate in the same direction and may well be additive.

Advection

The results obtained for the migration of ^{90}Sr under advective conditions tend to confirm the effect of CDP observed during diffusion, with an increased retardation of the radionuclide in the presence of the organic compounds. Modelling of the advection profiles resulted in a diffusivity value of 4.4×10^{-11} m^2 s^{-1} and a distribution coefficient of 2.7×10^{-3} m^3 kg^{-1}. However, the predicted elution profile does not fit well with the experimental values (Figure 6A); the breakthrough and peak concentration appear too early and the model shows higher dispersion (flatter and wider peak) than the experimental curve. When the same parameters were employed to model advection in the presence of CDP, the predicted curve matched the general shape of the peak very well (Figure 6B), although the cumulative elution of Sr for the model (area under the curve) was higher than observed experimentally. It was necessary to restrict the total inventory of ^{90}Sr (assuming 23% of the ^{90}Sr had precipitated or was in some way bound to the NRVB) to reproduce theoretically the advection data (also shown on Figure 6B). This reinforces the conclusion from the diffusion experiments that the organic compounds increase the retardation of Sr by NRVB.

Conclusion

The presence of CDP and/or an increase in ionic strength cause enhanced retention of Sr by the candidate repository backfill, NRVB. The effect could be explained by decalcification of the CSH phase that is primarily responsible for Sr retention. The results obtained here support a hypothesis of Ca ion-exchange as the main mechanism responsible for retardation of Sr. However, the fact that retention is reduced by the addition of carrier concentrations of Sr (non-active) would suggest that isotopic exchange with the intrinsic Sr already present in the cement paste may also play a role in the retention of ^{90}Sr. The reduced retardation at high concentrations is most likely explained by saturation of the retention sites. Slightly higher diffusivity values were obtained in the presence of gluconate ($D_e = 13 \times 10^{-11}$ m^2 s^{-1}), which suggest that the background level of Sr in the CDP solutions in comparison with NRVB-equilibrated water could have affected the diffusion process. Both diffusion and advection experiments show enhanced retardation with CDP and provide similar diffusivity and distribution coefficients for Sr onto NRVB, $D_e = 5.5 \times 10^{-11}$ - 8.5×10^{-11} m^2 s^{-1} and $R_d = 2.8 \times 10^{-3}$–3.1×10^{-3} m^3 kg^{-1}, in the absence of organic ligands.

Data availability statement

The raw data supporting the conclusion of this article will be made available by the authors, without undue reservation.

Author contributions

JH, MF-S, and NE contributed to conception and design of the study. JH completed the experimental work. JH carried out the initial evaluation of the data and DD performed the modelling. MF-S wrote the first draft of the manuscript. All authors contributed to manuscript revision, read, and approved the submitted version.

Funding

This research has been supported by the SKIN project, as part of the European Atomic Energy Community's Seventh Framework Programme (FP7/2007-2011).

Conflict of interest

Author DD was employed by WSP Golder.

The remaining authors declare that the research was conducted in the absence of any commercial or financial relationships that could be construed as a potential conflict of interest.

Publisher's note

All claims expressed in this article are solely those of the authors and do not necessarily represent those of their affiliated organizations, or those of the publisher, the editors and the reviewers. Any product that may be evaluated in this article, or claim that may be made by its manufacturer, is not guaranteed or endorsed by the publisher.

Supplementary material

The Supplementary Material for this article can be found online at: https://www.frontiersin.org/articles/10.3389/fnuen.2022.1042541/full#supplementary-material

References

Atkins, M., and Glasser, F. P. (1992). Application of portland cement-based materials to radioactive waste immobilization. *Waste Manag.* 12, 105–131. doi:10.1016/0956-053x(92)90044-j

Atkinson, A., Claisse, P. A., Harris, A. W., and Nickerson, A. K. (1989). Mass transfer in water-saturated concretes. *MRS Proc.* 176, 741–749. doi:10.1557/proc-176-741

Castellote, M., Andrade, C., and Alonso, C. (1999). Characterization of transport of caesium, strontium, cobalt and iron ions through concrete by steady-state migration and natural diffusion tests. *Adv. Cem. Res.* 11, 161–168. doi:10.1680/adcr.1999.11.4.161

Ciliberto, E., Condorelli, G. G., La Delfa, S., and Viscuso, E. (2008). Nanoparticles of Sr(OH)2: Synthesis in homogeneous phase at low temperature and application for cultural heritage artefacts. *Appl. Phys. A* 92, 137–141. doi:10.1007/s00339-008-4464-8

Coleman, N. J., Brassington, D. S., Raza, A., and Mendham, A. P. (2006). Sorption of Co^{2+} and Sr^{2+} by waste derived 11 Å tobermorite. *Waste Manag.* 26, 260–267. doi:10.1016/j.wasman.2005.01.019

Dezerald, L., Kohanoff, J. J., Correa, A. A., Caro, A., Pelleq, R. J.-M., Ulm, F. J., et al. (2015). Cement as a waste form for nuclear fission products; the case of ^{90}Sr and its daughters. *Environ. Sci. Technol.* 49, 13676–13683. doi:10.1021/acs.est.5b02609

Duchesne, J., and Reardon, E. J. (1995). Measurement and prediction of portlandite solubility in alkali solutions. *Cem. Concr. Res.* 25, 1043–1053. doi:10.1016/0008-8846(95)00099-x

Dudás, C., Kutus, B., Böszörményi, É., Peintler, G., Kele, Z., Pálinkó, I., et al. (2017). Comparison of the Ca^{2+} complexing properties of isosaccharinate and gluconate – is gluconate a reliable structural and functional model of isosaccharinate? *Dalton transactions. Dalton Trans.* 46, 13888–13896. doi:10.1039/c7dt03120c

El-Kamash, A. M., El-Naggar, M. R., and El-Dessouky, M. I. (2006). Immobilization of cesium and strontium radionuclides in zeolite-cement blends. *J. Hazard. Mat.* B136, 310–316. doi:10.1016/j.jhazmat.2005.12.020

Evans, N. D. M., Warwick, P., Felipe-Sotelo, M., and Vines, S. (2012). Prediction and measurement of complexation of radionuclide mixtures by α-isosaccharinic, gluconic and picolinic acids. *J. Radioanal. Nucl. Chem.* 293, 725–730. doi:10.1007/s10967-012-1828-5

Felipe-Sotelo, M., Hinchliff, J., Drury, D., Evans, N. D. M., Williams, S., and Read, D. (2014). Radial diffusion of radiocaesium and radioiodide through cementitious backfill. *Phys. Chem. Earth Parts A/B/C* 70-71, 60–70. doi:10.1016/j.pce.2014.04.001

Felipe-Sotelo, M., Hinchliff, J., Field, L. P., Milodowski, A. E., Holt, J. D., Taylor, S. E., et al. (2016). The solubility of nickel and its migration through the cementitious backfill of a geological disposal facility for nuclear waste. *J. Hazard. Mat.* 314, 211–219. doi:10.1016/j.jhazmat.2016.04.057

Felipe-Sotelo, M., Hinchliff, J., Field, L. P., Milodowski, A. E., Preedy, O., and Read, D. (2017). Retardation of uranium and thorium by a cementitious backfill developed for radioactive waste disposal. *Chemosphere* 179, 127–138. doi:10.1016/j.chemosphere.2017.03.109

Fuhrmann, M., Pietrzak, R., Heiser, J., Franz, E. M., and Colombo, P. (1989). The effects of temperature on the leaching behavior of cement waste forms - the cement/sodium sulfate system. *MRS Proc.* 176, 75–80. doi:10.1557/proc-176-75

Gaona, X., Dähn, R., Tits, J., Scheinost, A., and Wieland, E. (2011). Uptake of Np(IV) by C-S-H phases and cement paste: An EXAFS study. *Environ. Sci. Technol.* 45, 8765–8771. doi:10.1021/es2012897

Gashier, W., Miura, T., Hashimoto, K., Hand, R. J., and Kinoshita, H. (2014). Leaching behaviour of cementitious nuclear wasteforms containing caesium and strontium. *Adv. Appl. Ceram.* 113, 447–452. doi:10.1179/1743676114y.0000000146

Gelhar, F. W., Welty, C., and Rehfeldt, K. R. (1992). A critical review of data on field-scale dispersion in aquifers. *Water Resour. Res.* 28, 1955–1974. doi:10.1029/92wr00607

Glaus, M. A., Laube, A., and Van Loon, L. R. (2006). Solid–liquid distribution of selected concrete admixtures in hardened cement pastes. *Waste Manag.* 26, 741–751. doi:10.1016/j.wasman.2006.01.019

Glaus, M. A., and Van Loon, L. R. (2008). Degradation of cellulose under alkaline conditions: New insights from a 12 years degradation study. *Environ. Sci. Technol.* 42, 2906–2911. doi:10.1021/es7025517

Glaus, M. A., Van Loon, L. R., Schwyn, B., Vines, S., Williams, S. J., Larsson, P., et al. (2008). Long-term predictions of the concentration of alpha-isosaccharinic acid in cement pore water. *Mat. Res. Soc. Symp. p.* 1107, 605–612. doi:10.1557/PROC-1107-605

Goo, J.-Y., Kim, B.-J., Kang, M., Jeong, J., Jo, H. Y., and Kwon, J.-S. (2021). Leaching behavior of cesium, strontium, cobalt, and europium from immobilized cement matrix. *Appl. Sci. (Basel).* 11, 8418. doi:10.3390/app11188418

Hinchliff, J., Felipe-Sotelo, M., Evans, N. D. M., and Read, D. (2016). Solubility constraints affecting the migration of selenium through the cementitious backfill of a geological disposal facility. *J. Hazard. Mat.* 305, 21–29. doi:10.1016/j.jhazmat.2015.11.024

Isaacs, M., Lange, S., Deissmann, G., Bosbach, D., Milodowski, A. E., and Read, D. (2020). Retention of technetium-99 by grout and backfill cements: Implications for the safe disposal of radioactive waste. *Appl. Geochem.* 116, 104580. doi:10.1016/j.apgeochem.2020.104580

Iwaida, T., Nagasaki, S., and Tanaka, S. (2000). Sorption study of strontium onto hydrated cement phases using a sequential desorption method. *Radiochim. Acta* 88, 483–487. doi:10.1524/ract.2000.88.8.483

Johnston, H. M., and Wilmot, D. J. (1992). Sorption and diffusion studies in cementitious grouts. *Waste Manag.* 12, 289–297. doi:10.1016/0956-053x(92)90055-n

Keith-Roach, M. J. (2008). The speciation, stability, solubility and biodegradation of organic co-contaminant radionuclide complexes: A review. *Sci. Total Environ.* 396, 1–11. doi:10.1016/j.scitotenv.2008.02.030

Kittnerová, J., Drtinová, B., Štamberg, K., Vopálka, D., Evans, N., Deissman, G., et al. (2020). Comparative study of radium and strontium behaviour in contact with cementitious materials. *Appl. Geochem.* 122, 104713. doi:10.1016/j.apgeochem.2020.104713

Krishnamoorthy, T. M., Joshi, S. N., Doshi, G. R., and Nair, R. N. (1993). Desorption kinetics of radionuclides fixed in cement matrix. *Nucl. Technol.* 104, 351–357. doi:10.13182/nt93-a34896

Liu, J., Tang, K., Qiu, Q., Pan, D., Lei, Z., and Xing, F. (2014). Experimental investigation on pore structure characterization of concrete exposed to water and chlorides. *Materials* 7, 6646–6659. doi:10.3390/ma7096646

Ma, W., Brown, P. W., and Komarneni, S. (1996). Sequestration of cesium and strontium by tobermorite synthesized from fly ashes. *J. Am. Ceram. Soc.* 79, 1707–1710. doi:10.1111/j.1151-2916.1996.tb08790.x

Markovaara-Koivisto, M., Read, D., Lindberg, A., Siitari-Kauppi, M., and Marcos, N. (2008). "Uranium mineralogy at the Askola ore deposit, Southern Finland," in Mater. Res. Soc. Symp. , Massachusetts, USA, 1-5 December 2008. 1124-Q10-02.

Merz, E. R., Dyckerhoff, D., and Odoj, R. (1987). Characterization of radioactive wastes incorporated in a cement matrix. *Nucl. J. Can.* 1, 173–178.

Morgan, M. T., McDaniel, E. W., Moore, J. G., Devaney, H. E., and Dole, L. R. (1982). Strontium leachability of hydrofracture grouts for sludge-slurries. Report ORNL/TM-8198.

Nuclear Decommissioning Authority. (2010b). Geological disposal. Generic post-closure safety assessment. NDA report No NDA/RWMD/030.

Nuclear Decommissioning Authority. (2010a). Geological disposal. Near–field evolution status report. NDA report No NDA/RWMD/003.

Ochs, M., Colàs, E., Grivé, M., Olmeda, J., Campos, I., and Bruno, J. (2014). Reduction of radionuclide uptake in hydrated cement systems by organic complexing agents: Selection of reduction factors and speciation calculations. SKB report No R-14-22.

Pallagi, A., Bajnóczi, É. G., Canton, S. E., Bolin, T., Peintler, G., Kutus, B., et al. (2014). Multinuclear complex formation between Ca(II) and gluconate ions in hyperalkaline solutions. *Environ. Sci. Technol.* 48, 6604–6611. doi:10.1021/es501067w

Pointeau, I., Coreau, N., and Reiller, P. E. (2008). Uptake of anionic radionuclides onto degraded cement pastes and competing effect of organic ligands. *Radiochim. Acta* 96, 367–374. doi:10.1524/ract.2008.1503

Putero, S. H., and Rosita, W. (2013). Performance of cement for immobilizing strontium waste in saline environment. *Mat. Sci. Appl.* 4, 7–11. doi:10.4236/msa.2013.412a002

Putero, S. H., Rosita, W., Santosa, H. B., and Budiarto, R. (2013). The performance of various pozzolanic materials in improving quality of strontium liquid waste cementation. *Procedia Environ. Sci.* 17, 703–710. doi:10.1016/j.proenv.2013.02.087

Shackelford, C. D., and Moore, S. M. (2013). Fickian diffusion of radionuclides for engineered containment barriers: Diffusion coefficients, porosities, and complicating issues. *Eng. Geol.* 152, 133–147. doi:10.1016/j.enggeo.2012.10.014

Shiner, M. E., Klein-BenDavid, O., L'Hôpitall, E., Dauzères, A., Neji, M., Teutsch, N., et al. (2022). Retention of strontium in high- & low-pH cementitious matrices – OPC vs. model systems. *Cem. Concr. Res.* 152, 106659. doi:10.1016/j.cemconres.2021.106659

Shrivastava, O. P., and Shrivastava, R. (2000). Cation exchange applications of synthetic tobermorite for the immobilization and solidification of cesium and strontium in cement matrix. *Bull. Mat. Sci.* 23, 515–520. doi:10.1007/bf02903893

Shrivastava, O. P., and Shrivastava, R. (2001). Sr^{2+} uptake and leachability study on cured aluminium-substituted tobermorite-OPC admixtures. *Cem. Concr. Res.* 31, 1251–1255. doi:10.1016/s0008-8846(01)00567-1

Shrivastava, O. P., and Verna, T. (1995). Sr^{2+} sorption and leach rate studies on synthetic calcium silicate hydroxyl hydrate. *Adv. Cem. Based Mat.* 2, 119–124. doi:10.1016/1065-7355(94)00032-8

Tasi, A., Gaona, X., Rabung, Th., Fellhauer, D., Rothe, J., Dardenne, K., et al. (2021). Plutonium retention in the isosaccharinate – cement system. *Appl. Geochem.* 126, 104862. doi:10.1016/j.apgeochem.2020.104862

Tits, J., Wieland, E., Dobler, J. P., and Kunz, D. (2004). The uptake of strontium by calcium silicate hydrates under high pH conditions: An experimental approach to distinguish adsorption from co-precipitation processes. *MRS Proc.* 807, A101–A694. doi:10.1557/proc-807-a101

Tits, J., Wieland, E., Müller, C. J., Landesman, C., and Bradbury, M. H. (2006). Strontium binding by calcium silicate hydrates. *J. Colloid Interface Sci.* 300, 78–87. doi:10.1016/j.jcis.2006.03.043

Tsutsumi, T., Nishimoto, S., Kameshima, Y., and Miyake, M. (2014). Hydrothermal preparation of tobermorite from blast furnace slag for Cs^{+} and Sr^{2+} sorption. *J. Hazard. Mat.* 266, 174–181. doi:10.1016/j.jhazmat.2013.12.024

van Es, E., Hinchliff, J., Felipe-Sotelo, M., Milodowski, A. E., Field, L. P., Evans, N. D. M., et al. (2015). Retention of chlorine-36 by a cementitious backfill. *Mineral. Mag.* 79, 1297–1305. doi:10.1180/minmag.2015.079.6.05

Van Loon, L. R., and Glaus, M. A. (1998). *Experimental and theoretical studies on alkaline degradation of cellulose and its impact on the sorption of radionuclides*. Villigen, Switzerland: Paul Scherrer Institute. PSI report 98-07.

Vercammen, K., Glaus, M. A., Van Loon, L. R., Ghosh, S., Andersson, P. G., Moller, J., et al. (1999). Complexation of calcium by α-isosaccharinic acid under alkaline conditions. *Acta Chem. Scand.* 53, 241–246. doi:10.3891/acta.chem.scand.53-0241

Wallace, S. H., Shaw, S., Morris, K., Small, J. S., Fuller, A. J., and Burke, I. T. (2012). Effect of groundwater pH and ionic strength on strontium sorption in aquifer sediments: Implications for ^{90}Sr mobility at contaminated nuclear sites. *Appl. Geochem.* 27, 1482–1491. doi:10.1016/j.apgeochem.2012.04.007

Wieland, E. (2014). Sorption data base for the cementitious near field of L/ILW and ILW repositories for provisional safety analyses for SGT-E2. Nagra report No 14-08.

Wieland, E., Tits, J., Kunz, D., and Dähn, R. (2008). Strontium uptake by cementitious materials. *Environ. Sci. Technol.* 42, 403–409. doi:10.1021/es071227y

Yarusova, S. B., Gordienko, P. S., Krysenko, G. F., and Azarova, Y. A. (2014). Sr^{2+} sorption by synthetic and technogenic silicate material. *Inorg. Mat.* 50, 599–605. doi:10.1134/s002016851406020x

Youssef, M., Pelleq, R. J.-M., and Yildiz, B. (2014). Docking ^{90}Sr radionuclide in cement: An atomistic modeling study. *Phys. Chem. Earth Parts A/B/C* 70-71, 39–44. doi:10.1016/j.pce.2013.11.007